

LEGGED ROBOT LOCOMOTION IN RESISTIVE TERRAIN: A COMPARISON OF TWO METHODS

MIKULAS SZABARI, RADEK KNOFLICEK

*Institute of production machines, systems and robotics, Faculty
of mechanical engineering, Brno university of technology,
Brno, Czech Republic*

DOI: 10.17973/MMSJ.2022_11_2022047

Mikulas.Szabari@vutbr.cz, knoflicek@fme.vutbr.cz

Every day new technology appears. In the field of legged robots, it is not otherwise. LIDAR vision, artificial intelligence, computing power and new drives help to improve the state of legged robots. One of the unsolved problems is still terrain navigation, such as locomotion in resistive terrain. To determine the correct locomotion, research must be carried out. In this paper, we compare two different situations, where a six-legged robot walks through variable resistive terrain with different gait in the first one and with different leg trajectories in the swing phase in the second one.

KEYWORDS

legged robot, resistive terrain, robot gait, leg retraction, Matlab Simulink

1 INTRODUCTION

Terrain overcoming is one of the basic demands for legged robots. They should be able to walk in uneven, unstable and high gradient terrain, but also in resistive terrain. Resistive terrain is described as a rigid ground layer covered by a layer of a resistive continuum of an arbitrary depth [Gart 2021]. The example of this terrain is shallow water, sand, mud, snow and tall grass. The novelty of this terrain for legged robots is consistent resistance acting on their legs or on the robot body itself in any direction, and the legged robots need to deal with them.

Legged robots have numerous parameters, which can be controlled. One of them is gait. Gait is a pattern which defines when and how long each leg has contact with the ground in a certain order. In general, animals choose gait based on actual speed, terrain, manoeuvre, energetic efficiency or operation. This adaptation is replicated by legged robots too. For example, hexapod robot Hexa V4 switches between two gaits based on its actual speed to reach better energy efficiency [Luneckas 2021]. Similarly, we could switch several gaits to reach higher speed or energy efficiency in variable resistive terrain.

An important part of walking is the leg trajectory. The leg trajectory is divided into two sections which correspond to leg phases: the support phase, where a leg has contact with the ground, and the swing phase, where a leg is in free space. The leg trajectory in the support phase is constant and depends on the surface. On the other hand, the leg trajectory in the swing phase has more possibilities. In general, the leg trajectory in the swing phase consists of these three parts: losing contact, reverse motion and initial contact. The shape of reverse motion is different based on the demanded application. To achieve high robot speed, different oval leg trajectories were developed [Ko 2010]. For crossing a wide ditch, the circular and the straight trajectories were used [Janardhan 2017]. The parabolic shape was used to reduce energy consumption [Yang 2019] or overstep obstacles [Guo 2016]. Stair climbing is challenging for legged

robots and requires a special leg trajectory as well [Park 2010]. In case of resistive terrain, the developed shape of leg trajectory contains the retraction and trajectory is not presented by a simple geometric shape [Gart 2021]. The shape depends on the resistant fluid level and on demanded speed. The tested trajectories use either no retraction, 30% retraction or experimental retraction to increase speed and decrease energy consumption of a single-leg hopper.

The work presented in this paper compares two different approaches to improving resistive terrain navigation. The first method is based on switching gaits, which occurs when the robot evaluates his own state and chooses a new gait. The second known method works with leg trajectory as it was in the single-leg hopper [Gart 2021]. Unlike the study with the single-leg hopper, we use a six-legged robot. The design of the six-legged robot model is described in section 2.1. Section 2.2 a 2.3 is dedicated to the hexapod's gaits and leg trajectories. The description of resistive terrain and its parameters is in section 3. Section 4 is dedicated to the motion simulation and experiment with the six-legged robot with selected gaits and leg trajectories. The results of the simulation and experiment are summarized in section 5. Finally, section 6 forms the conclusion of this paper.

2 SIX-LEGGED ROBOT

2.1 Design and control

For the purpose of measurement, a hexapod robot model was designed. The selected hexapod is a crawl-type robot with even distributed legs in each corner of the hexagonal shaped body. The legs point out of the body centre in the base pose. Every leg has three links connected with three driven revolute joints, each of which has one DoF (degree of freedom). The orientation of joint axis is yaw, roll and roll and the length of link is $l_1=20.5$ mm, $l_2=41$ mm and $l_3=64$ mm from body to tip of the leg. A simplified graphic interpretation is in Fig. 1.

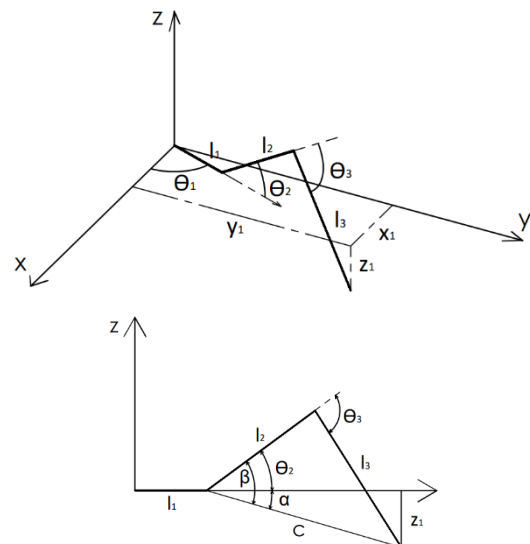


Figure 1. Kinematics of the leg

The relations between the location of the tip and zero points are as follows:

$$d = \sqrt{x_1^2 + y_1^2} - l_1 \quad (1)$$

$$c = \sqrt{z_1^2 + d^2} \quad (2)$$

$$\alpha = \text{atan}\left(\frac{z_1}{d}\right) \quad (3)$$

$$\beta = \text{acos}\left(\frac{c^2 + l_2^2 - l_3^2}{2l_2c}\right) \quad (4)$$

$$\theta_1 = \text{atan}\left(\frac{x_1}{y_1}\right) \quad (5)$$

$$\theta_2 = \alpha - \beta \quad (6)$$

$$\theta_3 = -\text{acos} \left(\frac{c^2 - l_2^2 - l_3^2}{2l_2l_3} \right) \quad (7)$$

where Θ_1 , Θ_2 and Θ_3 are the joint positions, and x_1 , y_1 , z_1 are coordination of tip of leg to zero point of coordination system.

The final graphical design of the whole robot is in Fig. 2a. The robot model was generated in the Matlab Simulink Simscape Multibody and scheme is shown on Fig. 2b. The robot consists of a body, which is the extruded solid hexagon located in the top centre of the Fig. 2b, and of six legs, which are each presented by blocks on the left and right. The body and legs are connected by reference frame connections, where the starting points are on each corner of hexapod body. The body and legs are connected by reference frame connections, where the starting points are on each corner of hexapod body. The schematic interpretation of a leg block is in Fig. 2c. The leg consists of two solid bricks and one cylinder connected by three revolute joints. The Fig. 2c also consist of eight rigid transformations to relocate and reorient the frames between the body and the joints. The tip of the legs is a non-dimensional sphere to simplify the calculation of the contact between the tip of the leg and the solid layer of resistive terrain. The control of the robot is by 18 data structure content of time and position of each degree of freedom. The calculation of these 18 structures was performed by an auxiliary program. The auxiliary program controls the robot by selected gait and leg trajectory.

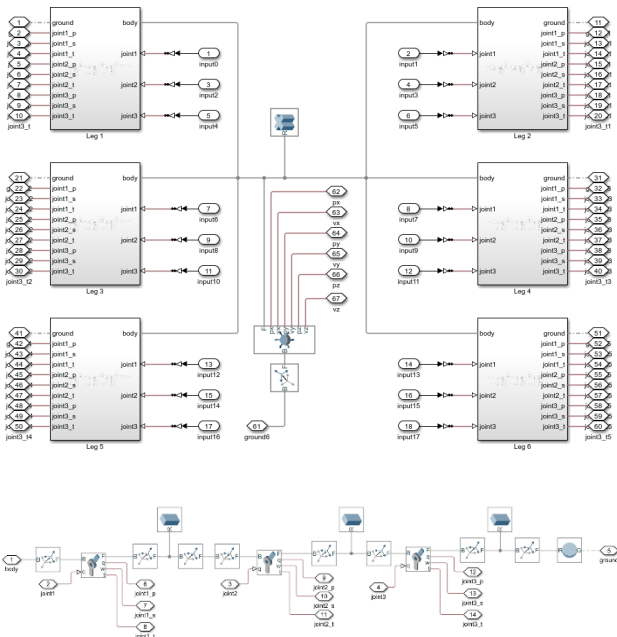
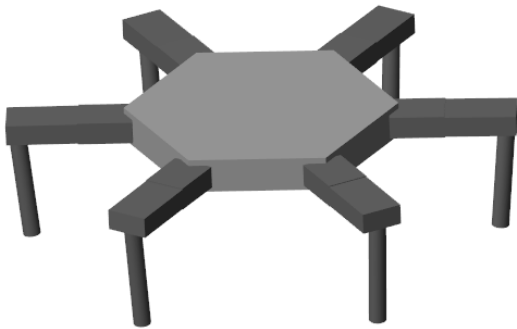
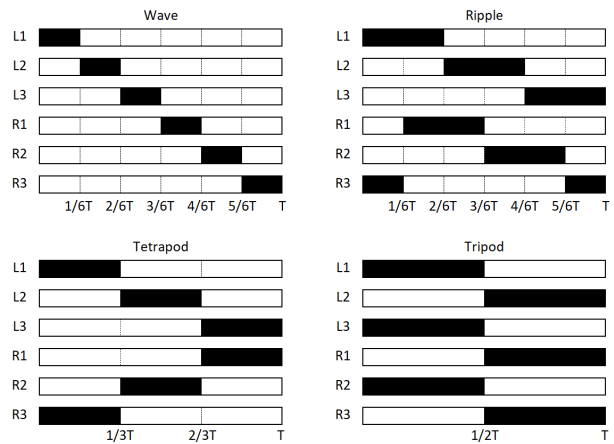


Figure 2. Hexapod robot model

2.2 Gait

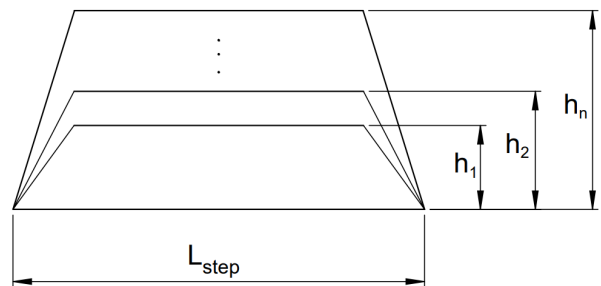
A hexapod robot has numerous gaits. For this work only four basic gaits were used. The four basic gaits the for hexapod are: wave, ripple, tetrapod and tripod gait. Each of these gaits has a different leg order and duration of ground contact. The timetable of these periodic gaits is displayed in Fig. 3. The wave gait uses one-sixth of the period to relocate the leg to a new start position. The ripple gait uses one-third of the period, same as the tetrapod gait. The tripod gait uses half of the period to relocate the leg. The differences in period length mean different time duration, therefore the reverse speed of leg. The reverse speed is six times as fast as the body of the robot for the wave gait, three times as fast for the ripple and tetrapod gait, and twice as fast for the tripod gait. The reverse speed is important due to drag forces which consist of a square of this speed.

The gait was implemented in simulation by an auxiliary program. The auxiliary program set the leg state by timetable and actual time for the selected gait.



2.3 Reverse leg trajectory

As mentioned above, the leg trajectory is divided into two parts by the leg phase. The trajectory where the leg is in the swing phase is named reverse leg trajectory. For this experiment, an isosceles trapezoid was selected as the shape of the leg trajectory from the robot's perspective. The base edge of the trapezoid represents the leg trajectory in the support phase, where leg has contact to ground. The other three edges represent the reverse leg trajectory. The height of the trapezoid is the same as the leg clearance (distance between ground and leg) and the length of base is the step length. To replicate the retraction method, we used the height of the trapezoid as a variable. The graphical representation of the trapezoids is shown in Fig. 4, where L_{step} stands for length step and h_1 to h_n stand for leg clearance.



3 RESISTIVE TERRAIN

The model of resistive terrain consists of two horizontally separated layers. The bottom layer works as a rigid ground and the upper layer is a resistive continuum, i.e. a density variable liquid in this experiment. The model of these two layers are Brick blocks in the Matlab Simulink environment. The rigid ground is 50 mm thick, 3 000 mm wide and 3 000 mm long. The liquid layer is 32 mm thick and has the same width and length as the rigid ground. The Brick block only works as geometrical space to evaluate the interaction between the layers and the robot legs. The interaction is provided by the Contact force block which calculates the actual position and speed of the selected point of a leg in the liquid layer. Inputs for this block are equations of axial and radial forces acting on the leg. The axial force is the sum of hydrostatic force calculated from the leg location in the liquid layer and the drag force calculated from the actual vertical speed of the leg in the liquid layer. The radial force is only drag force calculated from actual horizontal speed. The general equations are:

$$F_{ha} = p_h A_{ha} = \rho_l g h_s A_{ha} \quad (8)$$

$$F_{da} = \frac{1}{2} \rho_l v_a^2 C_{Da} A_{da} \quad (9)$$

$$F_{dr} = \frac{1}{2} \rho_l v_r^2 C_{Dr} A_{dr} \quad (10)$$

where F_{ha} is an axial hydrostatic force, p_h is a hydrostatic pressure, A_{ha} is the area of the leg profile in vertical direction, ρ_l is liquid density, g is gravitational acceleration, h_s is the submerged leg length, F_{da} is an axial drag force, v_a is the axial speed of a leg, C_{da} is an axial drag coefficient, A_{da} is the area of the leg profile in horizontal direction, F_{dr} is a radial drag force, v_r is the radial speed of the leg, C_{dr} is a radial drag coefficient and A_{dr} is the radial area of the leg.

The interaction of the rigid ground and the end of the leg provides the same Contact force block. In this case, the interference between the leg and the ground causes a normal force, which is calculated as two parts connected with a spring and a damper and a tangential force, which is calculated as the multiplication of the friction coefficient and the normal force. The friction coefficient has two parameters, static and dynamic, and they are chosen by an adjustable limit speed, which is compared with the actual speed provided by the Contact force block. Both friction parameters, limit speed, stiffness and damping can be set.

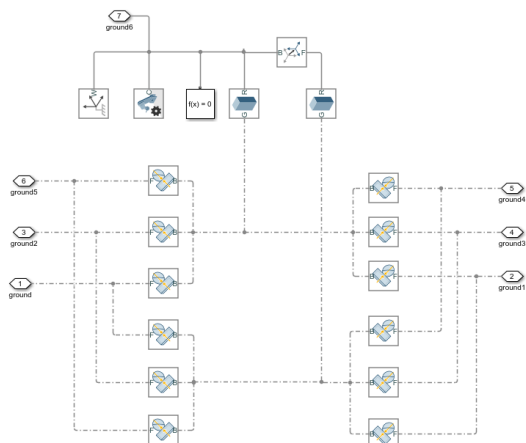
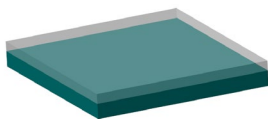


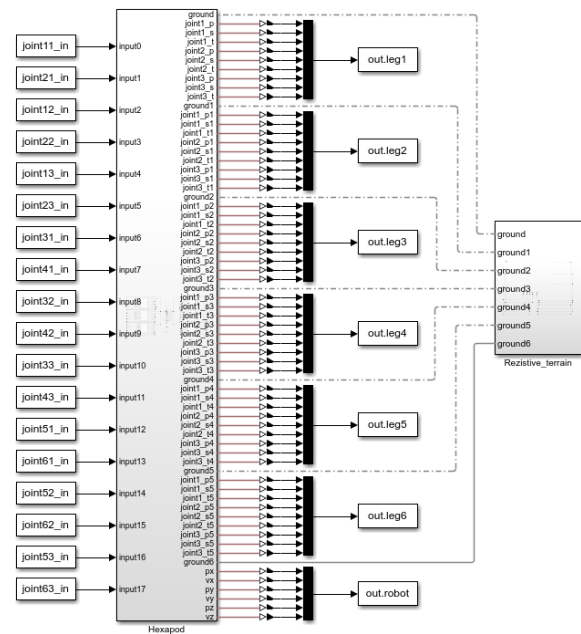
Figure 5. Model of resistive terrain

The graphical and schematic representation of the model is in Fig. 5. In the graphical interpretation, the green layer is the rigid ground covered by a semi-transparent white liquid layer. The schematic interpretation contains two Brick blocks connected by a Frame transform block and twelve Contact force blocks. Six of them deal with the contact between the rigid ground and the end of the legs and the other six deal with the contact between the liquid layer and the end arm of the legs.

4 SIMULATION AND EXPERIMENT

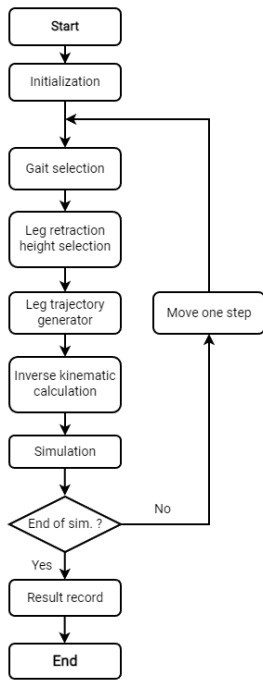
The selected simulation environment was Matlab Simulink Simscape Multibody [8], a setup to calculate inverse dynamics models. The hexapod robot and resistive terrain were imported into this simulator as shown in Fig. 2b and Fig. 5b. The resistive terrain and the end of the legs were connected by the Contact force block and also the body of the robot was connected to the zero frame of the resistive terrain by a 6-Dof Joint Block to set a default position of the body at the beginning of the simulation. The 6-Dof Joint Block allows free movement of the body and evaluates the distance and orientation between these two parts.

The overall model is shown in Fig. 6. On the left, there are inputs for individual joints connected to the hexapod robot block created from robot model in Fig. 2b. To the right of robot block, there are obtained outputs from the legs and the robot body. On the right, there is a block of environment created from the resistive terrain in Fig. 5b.



4.1 Control algorithm

The auxiliary program works as shown in Fig. 7. The first step is initialization, where all parameter and constant are loaded as in 4.2. The next steps are the gait and leg retraction height selection. These are selected by the user for the first time and repeatedly uploaded by a programable condition of the current method. The algorithm continues with the leg trajectory generator, which generates the time dependence position with a smooth curve of acceleration. The next steps are inverse kinematics and the simulation itself. After that, the state of simulation evaluates if the simulation is of its end; then the data is collected and the program ended. If not, the algorithm goes back to a point before the block gait selection and moves by one step.



4.2 Parameters

To run a simulation, the input parameters need to be determined. Tab. 1. lists all of the important parameters and constants for the simulation. The list contains dimensional and weight parameters of hexapod robots, duration of one gait period, dimension of the leg trajectory, resistive layer parameters and ground parameters.

Parameters	Notation	Value	Unit
Body length	l_b	0.134	m
Body width	w_b	0.155	m
Body mass	m_b	0.367	kg
Leg arm 1 length	l_1	0.021	m
Leg arm 1 mass	m_1	0.004	kg
Leg arm 2 length	l_2	0.040	m
Leg arm 2 mass	m_2	0.017	kg
Leg arm 3 length	l_3	0.064	m
Leg arm 3 mass	m_3	0.016	kg
Gait time period	T_{per}	1,2	s
Step length of wave gait	l_{stepw}	0.02	m
Step length of ripple gait	l_{stepr}	0.016	m
Step length of tetrapod gait	$l_{steppte}$	0.016	m
Step length of tripod gait	l_{steptr}	0.012	m
Gravitational acceleration	g	9.81	m/s^2
Axial drag coefficient	C_{Da}	0.47	-
Radial drag coefficient	C_{Dr}	0.47	-
Area of leg profile	A_{ha}	$3.14e^{-4}$	m^2
Area of leg profile	A_{da}	$3.14e^{-4}$	m^2
Ground stiffness	s_g	$1e^6$	N/m
Ground damping	d_g	$1e^4$	N/(m/s)
Static friction coefficient	f_c	0.2	-
Dynamic friction coefficient	f_d	0.15	-
Critical velocity	s_c	$1e^{-3}$	m/s

Table 1. Model parameters and constants

Tab. 2. determines the range of selected parameters. The range of the leg retraction is between 8 mm and 32 mm with an 8 mm step. These numbers correspond with 12.5%, 25%, 37.5% and 50% of the leg, respectively. The selected density is in the range between 0 kg/m^3 to 13 500 kg/m^3 , which corresponds, for example, with the density of mercury.

Parameters	Notation	Min. value	Max. value	Step	Unit
Density	ρ_l	0	13 500	500	kg/m^3
Leg retraction	H	0.008	0.032	0.008	m

Table 2. Range of parameters

4.3 Data collection and proposed method

In order to obtain information about the walking of the robot in the resistive terrain, initial experiments were performed. The first experiments tested all gait in a range of resistive terrains defined by density with a constant leg retraction. The other experiments test all leg retraction with the tripod gait in a range of resistive terrains defined by density. The density changes in steps as shown in Tab. 2 and a separate simulation was performed for each of them. The monitored values are the actual speed of the robot, the average vertical deviation of the robot body and the cost of transportation (CoT). This dimensionless cost of transportation measures how much energy it takes to move one kilogram of mass for one meter [Kim 2017]. The CoT is calculated as follows:

$$CoT = \frac{E}{mgd} \quad (11)$$

where m is the total weight of the robot, g is gravitational acceleration, d is the travelled distance and E is the total energy consumed by robot actuators with the formula:

$$E = \int_0^T P dt \quad (12)$$

where P is the physical power calculated as the multiplication of the actual torque and the actuator speed.

The obtained results are in Fig. 8. It displays the dependencies of speed, CoT and average vertical deviation in variable resistive terrain density of four different gaits on the left and on the right there are dependencies of four different leg retractions.

The measured data shows a deviation from the set speed at different gaits. The tripod gait reaches the smallest speed deviation in the range of density between 0 and 2500 kg/m^3 . In the range from 2500 to 13500 kg/m^3 , the smallest deviation is reached by both the wave and the tetrapod gaits. Although, the CoT of the wave gait is several times as high as that of the quadruped gait. The lowest CoT is exhibited by the tripod gait. The last monitored value is the vertical deviation, which increases in liquid thicker than 9 000 kg/m^3 . The measured data also show a speed loss of leg retraction. With increasing density, the speed loss for the submerged legs increases. The speed loss of a non-submerged leg is not influenced by density. The CoT depends on leg retractions and density; an 8 mm leg retraction has the lowest CoT for the density in the range from 0 to 2 000 kg/m^3 and about this density the lowest CoT is displayed by a 32 mm leg retraction. The last monitored value is the vertical deviation, which increases in liquid thicker than 10 000 kg/m^3 .

The proposed method to decrease the speed loss and increase the efficiency, in case of gaits, is gait switching. Based on the collected data, the decisive value for a gait switch is 17.5% of the speed loss, which is the crossing point for the tripod, ripple and wave gaits for these parameters and setup. The tripod gait has the minimal speed loss below 17.5% of the speed loss and tetrapod and wave have the minimal loss over 17.5% of the speed loss. The chosen gait for the speed loss over 17.5% is the tetrapod gait due to better CoT then the wave gait. The process

of gait switching is as follows: if the speed loss increases to 18%, the gait switches to tetrapod; if the speed loss decreases to 17%, the gait switches to tripod. The reason for not using 17.5% as a limit is due to a possible oscillation of gait switching.

In case of leg retraction, same as in [Gart 2021], we optimized the leg retraction to reach better CoT. The height of the leg retraction changes from 8mm to 32mm in the event of speed loss of more than 5%, which corresponds with the crossing of the CoT curve for the 8 mm and 32 mm retraction.

4.4 Comparison

Three simulations were performed to compare the leg retraction and the gait switching. In the first simulation, the gait and leg retraction were constants, and they were set to 8mm and tripod respectively. These values represent the control of legged robots with no optimization and they are commonly used for legged robots walking on flat surfaces with no specification demand for gait. In the second simulation, the gait switching was controlled by the proposed method and leg retraction was set to 8mm as in the first one. In the third simulation, the leg retraction method was applied and the tripod gait was used as in the first simulation. In this case, the leg retraction method was adapted to this study as mentioned in 4.2.

4.5 Simulation

The robot trajectory in simulation went through a variable density from 0 to 13 500 kg/m³, which is the same for the original leg retraction and gait switching. The ratio between the distance travelled and the density was linear and increased by 5 000 kg/m³ per meter. The distance travelled was therefore 2.7 meters. The other parameters were the same as in Tab. 1 and Tab. 2. The monitored values remained almost the same, and

they were speed of the robot, cost of transportation (CoT), vertical deviation of robot, with additional total time and energy consumed.

4.6 Experiment

For the purpose of confirmation, an experimental model and environment was built. The robot layout was same as in theoretical model. The six-legged robot was made from 18 MG90S servomotors and 3D printed frame and leg links. The dimensions and weights were preserved. The chosen control unit was Arduino Mega, which controlled all servomotors and measure flowing current, which powered them up. The power source was 8.4V Li-on battery, placed under the robot. The robot is shown in Fig. 9.

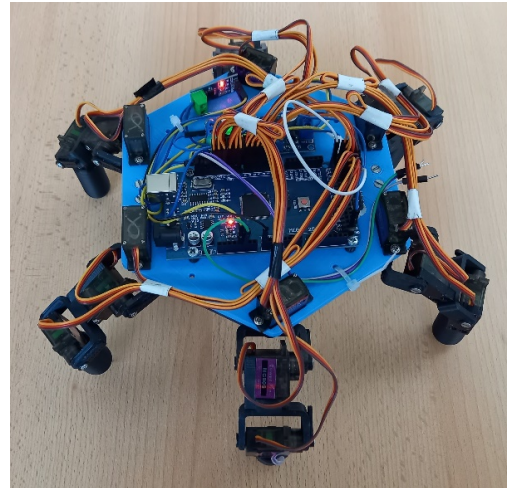


Figure 9. Experimental robot

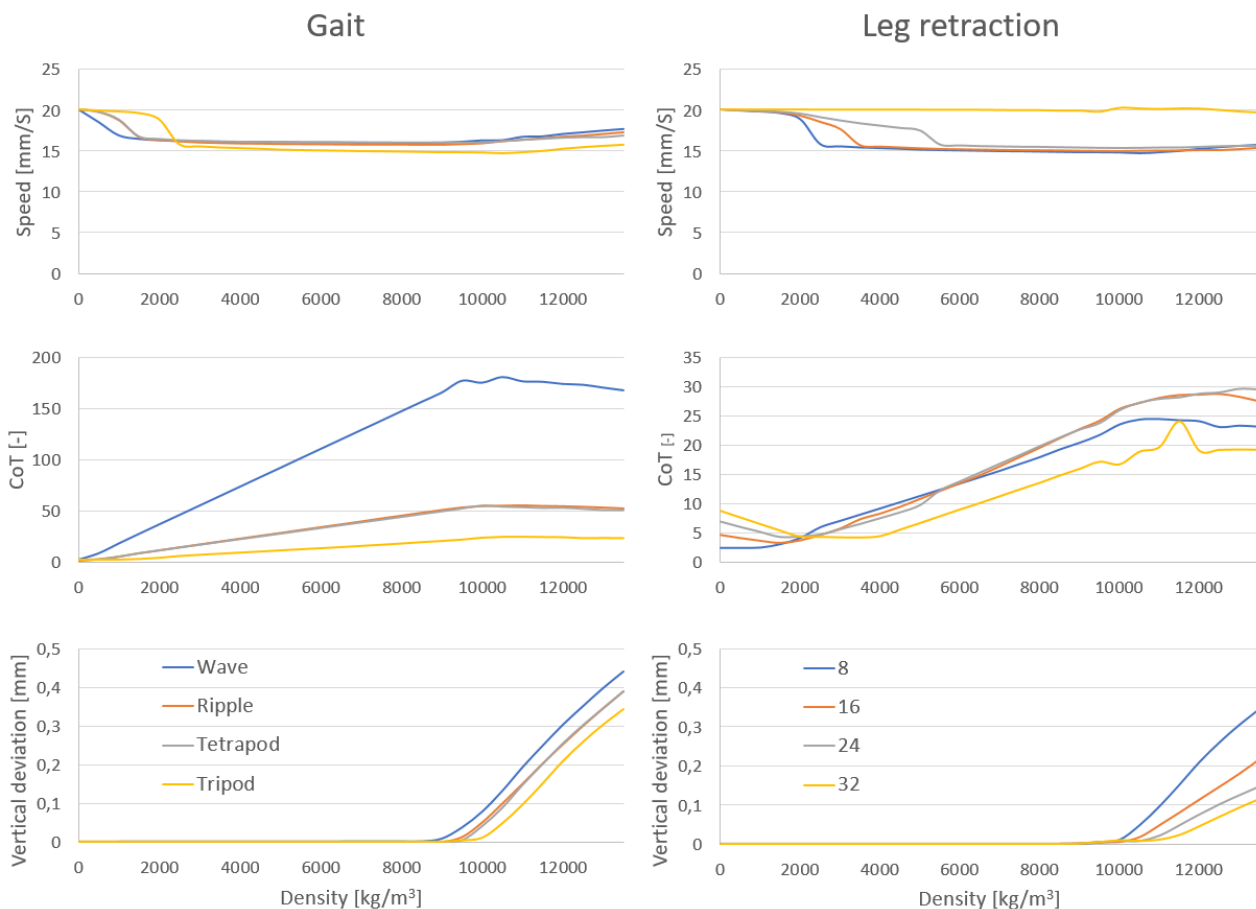


Figure 8. Initial experiment results

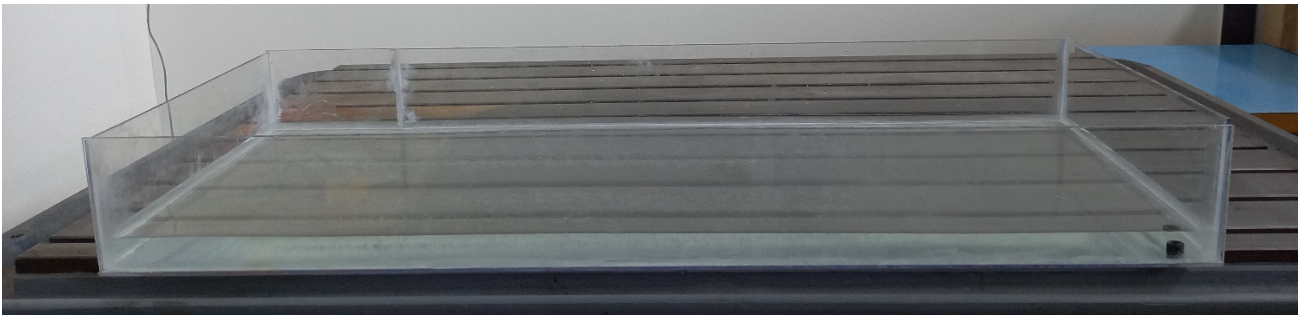


Figure 10. Container

The control of the robot was based on the simulation control. The motion of leg was regulated by state from gait timetable on Fig. 3. The recalculation between the Cartesian coordination and joint position was done by inverse kinematics in chapter 2.1. During the motion, the actual current was measured and recorded to evaluate the energy consumption of the robot.

The environment was represented by a rectangular container filled with water as shown in Fig. 10. The level of water was same as in simulation, i.e. 32 mm. The length, width and height of container was 1200 mm, 450 mm and 100 mm respectively.

The experiment consisted of seven measured movements of the hexapod, four measurements with four different gaits and 8 mm leg retraction and three measurements with the tripod gait and leg retraction height of 16, 24 and 32 mm. The path of hexapod was a straight line parallel to the longest side of container. The speed was set to 20mm/s and the walked distances were measured.

The experiment works only with constant water density equal to 1000kg/m³. The experiment was not performed in different liquid due to the toxicity of high-density liquid. Non-toxic fluid reaches approximately 2 000 kg/m³, which is not enough to observe gait switching or change of leg retraction.

The outcome of experiment were the speed and the CoT of individual measurements. The CoT was calculated in the same way as in formula 11 and 12, but the power was expressed as a product of voltage and actual current. The vertical deviation did

not occur in the density of 1000kg/m³, therefore was not included.

5 RESULTS

5.1 Simulation results

The simulation results are shown in Fig. 11. In the left upper corner is a graph of speed and density of the resistive terrain for all three simulations. The blue line shows the speed of the original setup with constant leg retraction and gait. The speed drops to approximately 0.015 after the density reaches more than 2 000 kg/m³ and remains at this value. From 11 000 kg/m³ the speed slightly increases. The orange line shows the speed of gait switching. The start of line is the same as the original due to the same parameters, but from 2 000 kg/m³ the speed shifts to approximately 0.016 and remains there. The shift is caused by gait change. The same as the original, the speed slightly increases at the end. The last grey line shows the speed of leg retraction. The start of the line is also the same. After reaching the density of 2 000 kg/m³, the speed gains value again, where the density is 0 kg/m³. When we compare these three lines, the start is the same for all of them. After the value of 2 000 kg/m³, the speed changes. In the case of the original, the drop is the biggest. The gait switching line shows a speed loss between the original and the leg retraction. The smallest speed loss is achieved by leg retraction. The improvement of gait switching compared to the original is around 7% and the leg retraction to the original is 33% after the value of 2 000 kg/m³.

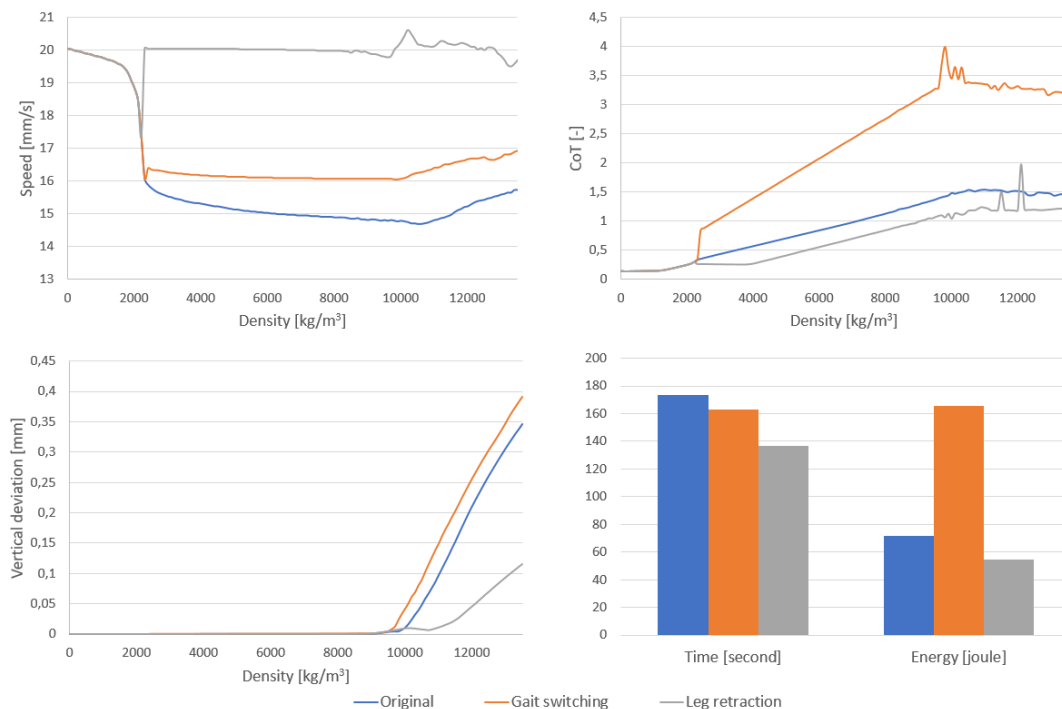


Figure 11. Results

Gait	Leg retraction height	Experimental speed [mm/s]	Simulated speed [mm/s]	Experimental CoT [-]	Simulated CoT [-]
Wave	8mm	18.0	16.9	8.62	17.9
Quadruped	8mm	18.9	18.9	8.58	5.2
Ripple	8mm	18.5	18.8	8.46	5.2
Tripod	8mm	19.3	19.8	8.27	2.4
Tripod	16mm	19.3	19.8	9.68	3.6
Tripod	24mm	19.9	19.9	12.7	5
Tripod	32mm	20.1	20	13.36	6.5

Table 3. Experimental results

Leg retraction is significantly better than gait switching in case of speed. In the right upper corner there is a graph of CoT and density. In the same way as speed, the CoT below the value of 2 000 kg/m³ is the same for all simulations due to the same parameters. The blue line represents the CoT of the original, and it increases near the end, where it remains at 1.5. Above the blue line, there is an orange line which represents gait switching. The line at the start shifts almost to value 1 and then increases more rapidly than the blue one. The last grey line represents the leg retraction. Out of all lines it reaches the lowest value, which means the best energy efficiency. The worst energy efficiency is reached by gait switching, which is even worse than the original.

The graph of vertical deviation and density is in the left bottom corner. Up to the density of 9 000 kg/m³, the deviation in the z axis is zero. The first of three simulations, in which deviation occur, is gait switching. The gait switching is represented by the orange line. Deviation of the original follows and they have the same course, but shifted to the right as the blue line shown. The last grey line represents the leg retraction and the course of deviation shows the slowest growth and the lowest value at the end. We can observe that the gait switch or change of leg retraction has no effect on the deviation. The deviation in the vertical axis occurs due to high density, and the robot swims in the resistive terrain for a moment when the toe of the leg reaches and moves away from the ground, even though the gait switching has a larger deviation than the original. The lowest reached deviation has leg retraction.

In the right bottom corner there is the total time and energy consumed from the CoT calculation. The total time was measured on a 2.7 m long trajectory. Both methods improve the total time; where the time of the original is 173 s, it is 163 s for gait switching and 136 s for leg retraction. The leg retraction time is improved compared to the original by 27%, where the improvement of gait switching is only 6%. The leg retraction is more than four times better.

The consumed energy on this trajectory is 72 J for the original, 166 J for gait switching, and 55 J for leg retraction. The amount of energy consumed by the gait switching is greater than for the original. The only improvement is reached by leg retraction, which is 31% better than original.

The leg retraction method reports better monitored values, such as speed, CoT, vertical deviation, time and energy consumed, than the original or the gait switching. The gait switching is better than original in case of speed and time.

5.2 Experimental results

The experimental results are shown in Table 3. Seven measurements were recorded. On the left there is the selected gait and leg retraction, and on the other there are results consisting of experimental and simulated speeds and CoT. The measure speed and CoT represent real values and could be

compared to simulation data in Fig. 5. The experimental and simulated speeds correspond to each other except for the wave gait where the difference is more than 1mm/s. In the case of CoT, the experimental and simulated data are different. In the experiment, the CoT of different gaits has almost the same value, but in simulation the values are on a large scale. However, the order from the smallest to largest is preserved. The data of different leg retraction heights have same order and with a correction factor could match each other. The difference is caused by a known reality gap. The simulation and reality will never match due to the impossibility to simulate non-linear and complex behaviour, such as friction, drive control, water flow and many others. Also, the evaluation of CoT is different for simulation and experiment, which could be one of the reasons of this deviation. The simulation works with mechanical energy and the experiment works with electrical energy, which is not included in simulation. The missing elements in simulation are PID regulation and internal mechanic of drive.

6 CONCLUSION

In this paper, we have compared two approaches to overcome variable resistive terrain. The first approach was based on gait switching, where the order of the legs and their duration of contact with ground change. The second approach used leg retraction to avoid resistive terrain and move the legs in free space. In addition, a real robot and environment was built to test and confirm simulation.

To compare these two approaches, a six-legged robot and resistive terrain were developed as models in Matlab Simulink Simscape Multibody. The interaction between robot and terrain was established by a new Contact force block for the derivation of forces between them calculated by the general formula of drag. The developed model was used to simulate all of the tests and measurements.

Both approaches were first tested to find out limit values to switch gait or increase leg retraction to works as optimized. In both cases the limit density value was around 2 000 kg/m³. The tetrapod and tripod gait were selected for gait switching, because they are more suitable than waves or ripple from the perspective of speed, CoT and vertical deviation for appropriate density. In case of leg retraction, the best two heights, 8 mm a 32 mm, were selected to be changed.

After finding limiting values and adapting both methods, the comparison of leg retraction and gait switching with the original setup was performed. The reason for creating the original setup was to set a baseline for comparison. The original setup used a tripod gait and 8 mm leg retraction throughout simulation. The trajectory of the robot in the simulation was set through variable resistive terrain with constant increasing density 5 000 kg/m³ per meter and the length of trajectory was 2.7 m. The result shows

that the leg retraction method presents the smallest speed loss, smallest CoT, lowest vertical deviation, shortest total time and energy consumption than the original and gait switching. The gait switching method results in only smaller speed loss and shorter time than the original. Overall, the leg retraction method is better than the gait switching method for these parameters and constants. The reason why gait switching is so energy inefficient is the reverse motion speed. The reverse speed of the tripod is one third slower than the reverse speed of the tetrapod.

A real experiment was executed to confirm simulation model. A hexapod robot and resistive terrain were designed and built. The chosen liquid for resistive terrain was only water due to the toxicity of high-density liquids. Therefore, the results of the measuring are only points, not course. Seven measurements, under this condition, took place and were compared to the simulation. In case of speed, the difference was minimal. The simulation and experiment data correspond to each other. The CoT of experiment and simulation exhibit different values. The main reason is the evaluation of different power and theoretical work simulation without PID regulation and internal mechanic of drive. Although the order of the value matches each other. In case of different leg retraction height, the values correspond more and they show some linear dependence. To achieve more precise values, the simulation should be upgraded and tested with a real model to ensure the same behaviour.

Future work will focus on other aspects of robot walking parameters within the context of resistive terrain, such as vertical deviation in high density terrain or PID regulation of robot drives. Other possibilities are applying deep reinforcement learning or evolution methods to teach legged robots to walk in variable resistive terrain and automatically recognize it. Machine learning could also improve resistive terrain navigation with combining the gait switching method and the leg retraction method.

REFERENCES

- [Gart 2021] Gart, S., et al. Legged locomotion in resistive terrains [online]. *Bioinspiration & biomimetics*, January 2021, vol. 16, no. 2, January 2021. Available from <https://doi.org/10.1088/1748-3190/abd011>. ISSN 1748-3182
- [Guo 2016] Guo, F. et al. Motion planning for humanoid robot dynamically stepping over consecutive large obstacles. *Industrial robot*, March 2016, vol. 43, no. 2, pp. 204-220, ISSN 0143-991X
- [Janardhan 2017] Janardhan, V. and Prasanth Kumar, R. Online trajectory generation for wide ditch crossing of biped robots using control constraints, *Robotics and autonomous systems*, November 2017, vol. 97, pp. 61-82, ISSN 0921-8890
- [Ko 2010] Ko, C. et al. Trajectory planning and four-leg coordination for stair climbing in a quadruped robot. *IEEE/RSJ International Conference on Intelligent Robots and Systems in Taiwan* 18-22 October 2010, IEEE, pp. 5335-5340, ISBN 9781424466740
- [Luneckas 2021] Luneckas, M. et al. Hexapod robot gait switching for energy consumption and cost of transport management using heuristic algorithms, *Applied sciences*, February 2021, vol. 11, no. 3, pp. 1-13, ISSN: 2076-3417
- [Park 2010] Park, C. et al. Trajectory generation and control for a biped robot walking upstairs. *International journal of control, automation, and systems*, 210, vol. 8, no. 2, pp. 339-351, ISSN: 1598-6446
- [Kim 2017] Kim, S. and Wensing, P. Design of Dynamic Legged Robots, *Foundations and Trends® in Robotics*, January 2017, vol. 5, no. 2, pp 117-190
- [The MathWorks Inc. 2022] The MathWorks Inc. *Matlab Simulink Simscape Multibody*. The MathWorks Inc. 2021, Boston [online]. 1994/2021. Available from <https://uk.mathworks.com/products/simscape-multibody.html>
- [Yang 2019] Yang, K. et al. Energy efficient foot trajectory of trot motion for hydraulic quadruped robot, *Energies (Basel)*, 2019, vol. 12, no. 13, p. 2514, ISSN: 1996-1073

CONTACTS:

Ing. Mikulas Szabari, doc. Ing. Radek Knoflicek Dr.
Institute of production machines, systems and robotics,
Faculty of mechanical engineering, Brno university of
technology
Technicka 2896/2, Brno, 616 69, Czech Republic
+420 541 142 446, +420 541 142 474
Mikulas.Szabari@vutbr.cz, knoflicek@fme.vutbr.cz
<https://www.uvssr.fme.vutbr.cz/>